nature photonics

Article

https://doi.org/10.1038/s41566-022-01107-7

Experimental observation of Berry phases in optical Möbius-strip microcavities

Received: 9 June 2022

Accepted: 13 October 2022

Published online: 22 December 2022

Check for updates

Jiawei Wang[1,2,3,11], Sreeramulu Valligatla[1,11], Yin Yin[1,4], Lukas Schwarz[1], Mariana Medina-Sánchez[1], Stefan Baunack[1], Ching Hua Lee[5], Ronny Thomale[6], Shilong Li[7] ✉, Vladimir M. Fomin[1,8], Libo Ma[1] ✉ & Oliver G. Schmidt[2,9,10]

The Möbius strip, a fascinating loop structure with one-sided topology, provides a rich playground for manipulating the non-trivial topological behaviour of spinning particles, such as electrons, polaritons and photons, in both real and parameter spaces. For photons resonating in a Möbius-strip cavity, the occurrence of an extra phase—known as the Berry phase—with purely topological origin is expected due to its non-trivial evolution in parameter space. However, despite numerous theoretical investigations, characterizing the optical Berry phase in a Möbius-strip cavity has remained elusive. Here we report the experimental observation of the Berry phase generated in optical Möbius-strip microcavities. In contrast to theoretical predictions in optical, electronic and magnetic Möbius-topology systems where only Berry phase π occurs, we demonstrate that a variable Berry phase smaller than π can be acquired by generating elliptical polarization of resonating light. Möbius-strip microcavities as integrable and Berry-phase-programmable optical systems are of great interest in topological physics and emerging classical or quantum photonic applications.

The Berry phase (also called the 'geometric phase'), a non-integrable phase factor originating from a non-trivial evolution of a physical system in parameter space[1], plays a fundamental role in various fields ranging from condensed matter physics[2,3], acoustics[4], high-energy physics[5], cosmology[6], quantum information[7] to optics[8]. In optics, the Berry phase can be acquired by the non-trivial evolution of either the polarization state or the wave vector in its corresponding parameter space, with purely topological origin[8–13]. Investigation of the manipulation of polarization states was pioneered by S. Pancharatnam, and the generated geometric phase is now also called the Pancharatnam–Berry phase[1,10]. Generation of a Berry phase based on wave-vector evolution has been explored by recording polarization rotations in the open light paths of helical[14–17] or out-of-plane curvilinear waveguides[18]. Notably, in recent years, the generation of the topologically protected Berry phase has also been studied in specially designed three-dimensional (3D) optical microcavities with light circulating along a closed path, for example in asymmetric whispering-gallery-mode microcavities[19], out-of-plane microrings[20] and microrings with embedded angular

[1]Institute for Integrative Nanosciences, Leibniz IFW Dresden, Dresden, Germany. [2]Research Center for Materials, Architectures and Integration of Nanomembranes (MAIN), Technische Universität Chemnitz, Chemnitz, Germany. [3]School of Electronic and Information Engineering, Harbin Institute of Technology (Shenzhen), Shenzhen, China. [4]School of Materials Science and Engineering, Jiangsu University, Zhenjiang, China. [5]Department of Physics, National University of Singapore, Singapore, Singapore. [6]Institute for Theoretical Physics and Astrophysics, University of Würzburg, Würzburg, Germany. [7]Light-Matter Interactions for Quantum Technologies Unit, Okinawa Institute of Science and Technology Graduate University, Okinawa, Japan. [8]Laboratory of Physics and Engineering of Nanomaterials, Department of Theoretical Physics, Moldova State University, Chişinău, Republic of Moldova. [9]Material Systems for Nanoelectronics, Chemnitz University of Technology, Chemnitz, Germany. [10]Nanophysics, Dresden University of Technology, Dresden, Germany. [11]These authors contributed equally: Jiawei Wang, Sreeramulu Valligatla. ✉e-mail: shilong.li@oist.jp; l.ma@ifw-dresden.de

https://doi.org/10.1038/s41566-022-01107-7

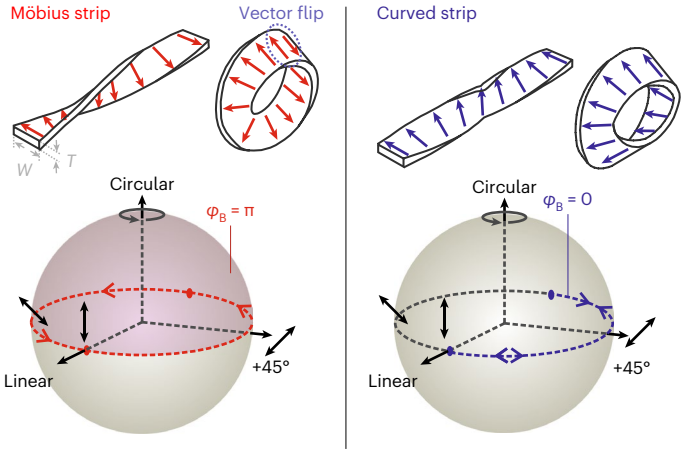

Fig. 1 | Berry phase occurring in Möbius- and curved-strip microcavities. Top: parallel transport of a vector along Möbius- and curved-strip cavities leads to a vector flip (occurrence of Berry phase π, dashed violet ellipse) and vector match (no Berry phase), respectively. Bottom: corresponding vector transport evolution on the Poincaré sphere with/without solid angle for the Möbius/curved strips.

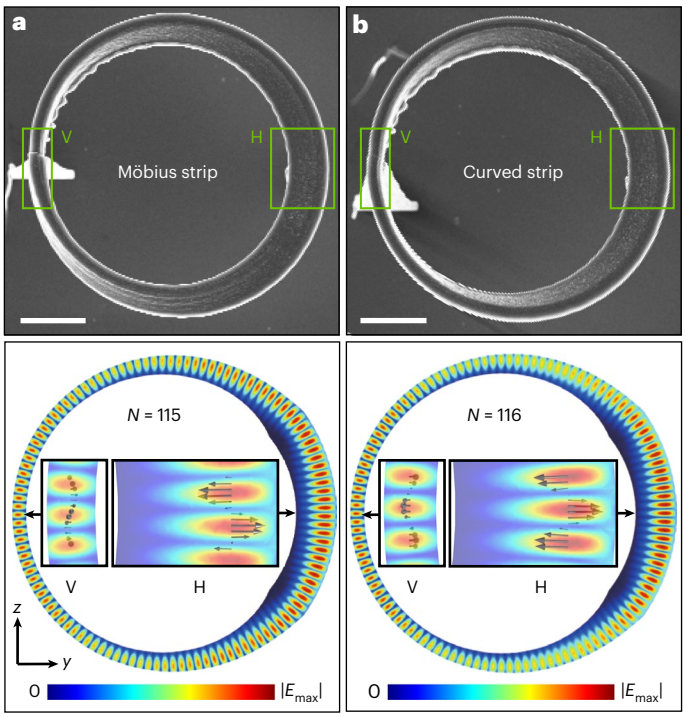

Fig. 2 | Optical resonant modes with and without Berry phase in Möbius- and curved-strip cavities. a,**b**, SEM images (top) of fabricated Möbius- (**a**) and curved-strip (**b**) cavities of the same size. Scale bars, 5 μm. The simulated optical-mode profiles (bottom) indicate that the polarization orientation of the resonant light rotates along the strip structure, generating the Berry phase. The presence/absence of the Berry phase leads to electric-field patterns with odd/even numbers of antinodes (cases with $N = 115$ and 116 are shown as examples) in the Möbius-/curved-strip microcavities. Insets: magnified images of the electric field at the vertical (V, where the strip is perpendicular to the substrate) and horizontal (H, where the strip is in parallel with the substrate) sites. Black arrows indicate the local polarization, revealing the rotation of the electric-field orientation along the cavities.

scatterers[21], which show great potential for on-chip integrated topological photonic devices.

The Möbius strip[22]—a fascinating loop structure well-known for its one-sided topology—also symbolizes the topological twist of the band structure in topological insulators[23]. The Möbius topology plays important roles in multiple disciplines, ranging from the generation of symmetry-breaking Möbius soliton modes in a magnetic medium[24] to the extraordinary behaviour of electronic waves in Möbius aromaticity[25] and twisted semiconductor strips[26], as well as anomalous plasmon modes formed in metallic Möbius nanostructures[27]. To impose the Möbius topology on photons, the optical field is twisted by liquid-crystal *q*-plates as cavity-free systems[28]. However, investigating the topological phenomena of light resonating in a real Möbius-structured cavity remains highly desirable. Very recently, a Möbius-strip cavity composed of a twisted dielectric strip was explored as a platform for the investigation of non-Euclidean optics[29]. However, the optical Berry phase, the key topological phenomenon, has not been experimentally demonstrated, although the existence of a Berry phase in a Möbius cavity was theoretically predicted a long time ago[30,31]. Theoretical studies have shown the occurrence of Berry phase π in an ideal Möbius-strip cavity, resulting in constructive self-interference of half-integer number modes (that is, accommodating half-integer numbers of wavelengths) in a closed-path trajectory[30]. The half-integer number of wavelengths, which has a purely topological origin, contradicts the well-known resonant condition in conventional optical or plasmonic cavities.

The topological behaviour of circulating light in Möbius-strip waveguiding systems has not yet been explored experimentally, preventing achieving new insights into observable optical phenomena for topology-based signal processing and communications. In this Article we report the experimental observation of optical Berry phases occurring in Möbius-strip microcavities with tailored cross-sectional geometry. In contrast to previous theoretical predictions, where only phase π occurs, here we observe and reveal programmable Berry phases ranging from π to 0 for resonant light waves with linear to elliptical polarization, in carefully designed Möbius-strip resonators. As the quantum holonomy, the Berry phase generated in a compact optical Möbius system is particularly promising for geometric quantum mechanics and its applications, such as simulation, metrology, sensing and computation.

Results

Principles

The discussion starts with the optical polarization states in an ideal Möbius strip, in which the strip thickness T is much smaller than the strip width W (Fig. 1). Considering linearly polarized light resonating in the Möbius-strip waveguide, the optical electric field is guided and forced to remain in the plane of the twisted strip. Such a twisted-strip waveguide functions similarly to some free-space optical components, such as a half-wave plate[1] or a Dove prism[32], which affect the orientation of the polarization states. As a result, the polarization continuously re-orients along the twisted strip during propagation, which we term the 'in-plane' (IP) mode. The IP mode represents an adiabatic cyclic evolution of linearly polarized light in a smoothly curved waveguide. The acquired phase factor of the light wave can be divided into two parts, the dynamic phase and the Berry phase (alternatively called the geometric phase). The dynamic phase reflects the system's evolution in time, which is determined by the optical path and the system's curvature. In contrast, the Berry phase memorizes the evolution path in the parameter space, which is independent of the dynamic phase. Using a phenomenological model, the occurrence of Berry phase in a Möbius strip can be directly visualized by the parallel transport of a vector along the twisted strip. For reference, we investigate a comparable 3D ring cavity ('curved strip') with the same curvature as that of a Möbius strip but without the Möbius topology (Supplementary Fig. 1 and Supplementary Note 1). In contrast to the one-sided Möbius strip with a single surface, the curved strip is topologically identical

https://doi.org/10.1038/s41566-022-01107-7

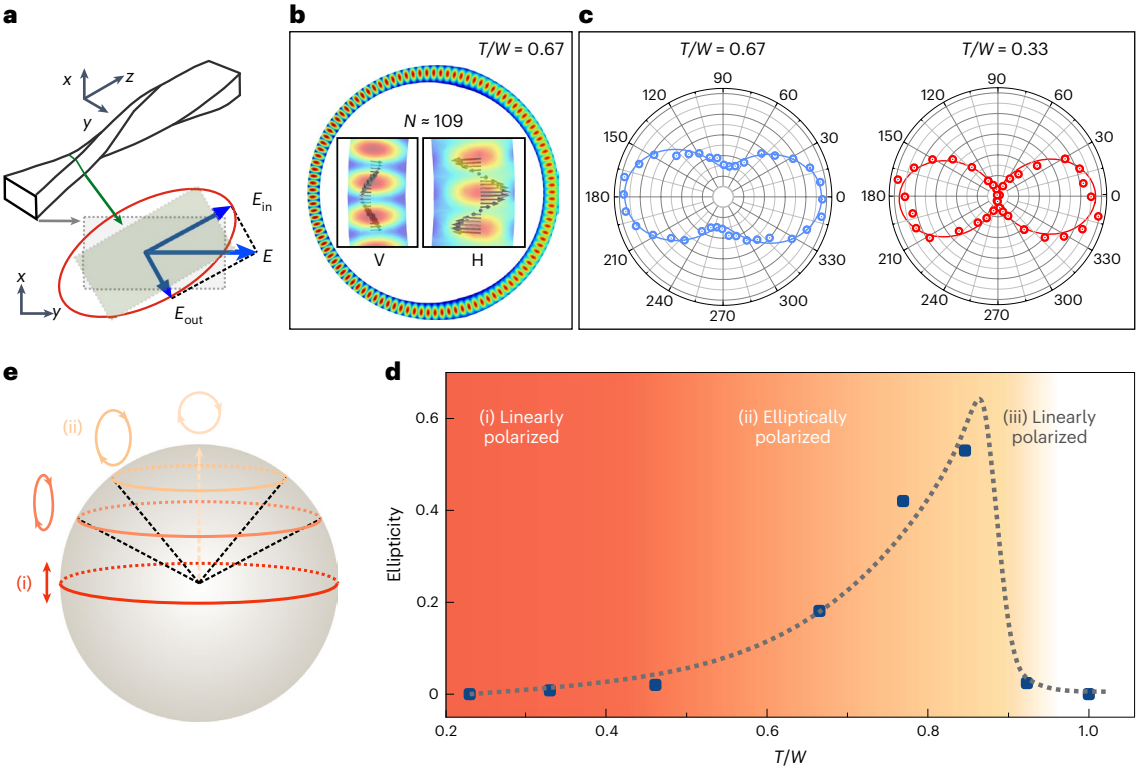

Fig. 3 | Variable ellipticity of resonant modes generated in Möbius-strip cavities. a, Linearly polarized light propagating along a twisted strip leads to the existence of in-plane and out-of-plane components and the formation of an elliptical polarization state. **b**, Cross-sectional views of the electric-field amplitude distributions for $T/W = 0.67$. Insets: magnified images of the electric field at the vertical and horizontal sites. Arrows indicate the local polarization. **c**, Polarization-resolved measurements for Möbius strips with $T/W = 0.33$ and 0.67. Dots, measured data; lines, sinusoidal fits. **d**, Summarized light ellipticity extracted from the simulated modes at the horizontal site of Möbius strips as a function of T/W. **e**, For simplicity, a cyclic evolution of the polarization state vector on a Poincaré sphere is used to describe the optical resonances in the Möbius strip, indicating that the occurring Berry phase directly depends on the ellipticity (represented by lines with arrows).

to conventional microring cavities. As shown in Fig. 1, although the vector orientations are kept in parallel with each other at each local position during transport, the vector flips by an angle π after a full trip around the Möbius strip, whereas there is no such a flip in the curved strip.

For the adiabatic cyclic evolution of a degenerate physical system there are usually two analytical ways to quantify the occurring Berry phase via the corresponding solid angle in parameter space. One way is determined by the wave vector **k**, which forms a sphere in momentum space. The Berry phase is equal to the solid angle enclosed by the trace of the wave vector at the origin of momentum space[14–16]. The other way is related to the wave polarization state vector, which spans the Poincaré sphere. The Berry phase is equal to half of the solid angle enclosed by the loop of the polarization vector at the origin of the Poincaré sphere[11,13].

For linear polarization, the polarization state can be described by $|s\rangle = \frac{1}{\sqrt{2}}(|+\rangle + |-\rangle)$, where $|+\rangle$ and $|-\rangle$ are right and left circular bases. The continuous variation of the polarization orientation can be visualized as a closed loop along the equator of the Poincaré sphere (Fig. 1, left), resulting in a solid angle, $\Omega = 2\pi$. Hence, a Berry phase as large as half the solid angle, $\Omega/2 = \pi$, is generated for the right and left circular polarization bases as $|s'\rangle = \frac{1}{\sqrt{2}}(e^{i\pi}|+\rangle e^{-i\pi}|-\rangle)$ (refs. [11–13]). For optical resonances in curved-strip cavities, the trajectory of the polarization evolution on the Poincaré sphere is topologically trivial and thus does not generate any Berry phase, as illustrated in Fig. 1. The similar photon propagation trajectory and propagation constant render the curved-strip cavity a perfect reference for our study of quantifying the Berry phase.

Light ellipticity in Möbius strips

Two-photon polymerization-based direct laser writing was used to fabricate dielectric Möbius- and curved-strip microrings using the negative photoresist IP-Dip (Methods and Supplementary Fig. 2). The polymerized IP-Dip is transparent in the visible to near-infrared spectral range, and is thus suitable for supporting optical resonances in this range. Figure 2a,b presents scanning electron microscopy (SEM) images of Möbius- and curved-strip cavities with identical design parameters, $T/W \approx 0.33$ ($T = 0.9$ μm).

To understand the behaviour of light propagation and resonances in all-dielectric Möbius microcavities, 3D numerical simulations based on the finite-element method were carried out (Methods). Figure 2 (bottom panels) presents the calculated mode profiles in typical Möbius and curved strips with $T/W = 0.33$ ($T = 0.9$ μm), respectively. The electric-field orientation of the resonant light rotates along the twisted strips, as can be seen in the magnified images of the horizontal and vertical sites of the Möbius and curved strips. In the Möbius-strip cavity, an odd number of antinodes ($N = 115$) is calculated, implying constructive interference with a half-integer mode number ($M = N/2 = 57.5$) of wavelengths. The constructive interference is off-phase in the case of half-integer numbers of wavelengths, and the phase mismatch is precisely compensated by the presence of Berry phase π, which leads to a 180° wave-flip. In the curved-strip cavity, the even number ($N = 116$) of antinodes corresponds to the conventional constructive interference with an integer number ($M = 58$) of wavelengths.

As a key approximation in an ideal Möbius strip, strip thickness T is assumed to be much smaller than the wavelength of the considered light in the waveguiding medium (λ/n), so the optical field is strictly

https://doi.org/10.1038/s41566-022-01107-7

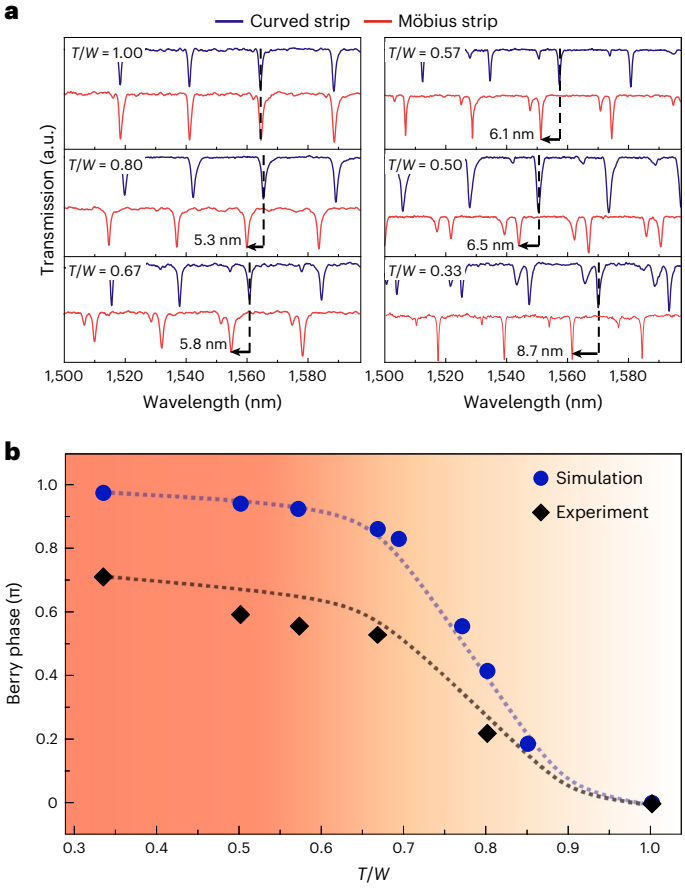

Fig. 4 | Polarization-dependent Berry phase as a function of the cross-section geometry, *T*/*W*. a, An increasing Berry phase is demonstrated by comparing the resonant-mode offsets between Möbius- and curved-strip cavities with decreasing *T*/*W*. The dashed lines and arrows are used to denote the wavelength offsets. **b**, Berry phase occurring in Möbius-strip cavities as a function of *T*/*W*. Circles and diamonds represent data extracted from experimental and simulated spectra, respectively. Dotted lines guide the eyes.

confined within the strip during propagation. In reality, the thickness of a Möbius-strip cavity can only be shrunk to a finite value, because of the need for sufficient optical confinement and low-loss light propagation. When *T* is comparable to *W*, the twisted cross-section does not provide rigorous in-plane confinement of the optical electric field. This leads to two competing effects. On the one hand, due to electromagnetic inertia, the electric field tends to maintain its orientation as it propagates along the strip. On the other hand, the tilted cross-section forces the electric field to rotate along the twisted strip. As a result, the main electric-field orientation tilts away from the strip plane, generating in-plane and out-of-plane components (Fig. 3a) with a phase retardation due to the different effective refractive indices for the electric-field components in and perpendicular to the strip plane (Supplementary Fig. 3 and Supplementary Note 1). An elliptical polarization is thus formed in the cross-section of the Möbius-strip cavity, as illustrated in Fig. 3a,b.

The resonant modes were characterized by measuring transmission spectra using an evanescently coupled tapered nanofibre—a widely adopted approach for near-field delivery and probing of light waves (Methods, Supplementary Fig. 4 and Supplementary Note 2)[33]. The polarization states of the resonant light in the Möbius- and curved-strip microcavities were examined by tuning the input optical polarization, step by step. For the Möbius-strip cavity with $T/W \approx 0.67$, the measurement shows an elliptical polarization state (Fig. 3c). This is in sharp contrast to the linear polarization state for the Möbius-strip cavity with $T/W \approx 0.33$. The ellipticity as a function of T/W was further studied by numerical simulations (Fig. 3d). The resonant light is almost linearly polarized when $T/W < 0.5$, and becomes elliptically polarized when $T/W > 0.5$. A further increase in T/W leads to a 'torus-like'-ring structure ($T/W \approx 1$). In this case, the optical electric field is no longer forced to rotate along the structure with a square-shaped core (Supplementary Fig. 6 and Supplementary Note 4), so the light does not undergo any non-trivial topological evolution.

The evolution of elliptically polarized resonant light projects a loop onto the Poincaré sphere away from the equator, depending on its ellipticity (Fig. 3e). With solid angle Ω changing between 2π and 0, Berry phase φ_B is generated for the right and left circular polarization bases as $|s'\rangle = \frac{1}{\sqrt{2}}(e^{i\varphi_B}|+\rangle + e^{-i\varphi_B}|-\rangle)$. Accordingly, by engineering the polarization ellipticity, one can develop a strategy to generate a variable Berry phase affecting both the eigenvalues and eigenstates of Möbius-strip cavities. For $T/W \approx 1$, the unmodified and non-rotating polarization state leads to the absence of the Berry phase, indicating a negligible Möbius-topology effect on the resonant light. Berry phase-involved constructive interferences in a Möbius strip are described further in Supplementary Note 5.

Manipulating Berry phases

Controlling the cross-sectional dimension of a Möbius waveguiding system provides great flexibility in supporting the optical resonances of elliptically polarized light and hence manipulating the acquired Berry phases. The acquired Berry phases are summarized in Fig. 4a by comparing the resonant modes measured in pairs of Möbius- and curved-strip cavities with various *T*/*W* values (Methods). In the case of $T/W = 1$, no wavelength offsets are observed between the Möbius- and curved-strip cavities, indicating the absence of the extra phase, that is, the Berry phase. As *T*/*W* decreases, clear increasing resonant-mode offsets emerge in the resonant spectra measured for the Möbius- and curved-strip cavities, providing direct evidence of an increasing Berry phase acquired in the Möbius-strip samples.

The simulation results in Fig. 4b reveal a consistent trend and confirm that the Berry phase can be freely tuned in the range from π to 0 by shaping the waveguiding cross-section of a Möbius strip. *T*/*W* ratios ranging between ~0.65 and ~0.85 are well suited to tuning the Berry phase, as the ellipticity of the resonant light is particularly sensitive to *T*/*W* in that range. The Berry phase φ_B extracted from the resonant-mode spectra is slightly lower than that derived from simulations over the whole *T*/*W* ratio range, as the measured resonant-mode offsets are not as large as those from theoretical calculations. In an ideal case, the resonant-mode offset is solely determined by the presence of the Berry phase, and the Möbius- and curved-strip cavities generate an identical dynamic phase as a result of having the same size and curvature. In practical sample fabrication, a substantial curvature discrepancy exists between the Möbius- and curved-strips due to the structural-symmetry-induced inherent strain, which reduces the mode offsets for the two types of cavity. As such, a deviation between experimental and simulated phase values constantly exists in the entire investigated *T*/*W* ratio range except for $T/W = 1$, showing the same evolution trend of Berry phase as a function of *T*/*W*.

Discussion

The above mainly focuses on circulating light with an optical electric field parallel to the strip plane (IP modes). However, resonant modes with an optical electric field perpendicular to the strip plane, termed 'out-of-plane' (OP) modes, can also be well supported for generation of the Berry phase at sufficiently large values of *T*. Similar to IP modes, OP modes with linear and elliptical polarizations can be formed for the generation of a variable Berry phase. Simulation and experimental results for OP modes and the associated Berry phases, presented in Supplementary Figs. 8 and 9 and Supplementary Notes 6 and 7, show similar behaviour to IP modes.

As a topological effect arising in cyclic adiabatic evolution, Berry phases for photons have been observed and systematically investigated using all-dielectric optical Möbius-strip cavities. The variable cross-section of the waveguiding strip produces different responses of light towards the twisted topology. Curved-strip cavities with the same curvature were taken as a topologically trivial counterpart to extract the Berry phase. By controlling the cross-sectional strip dimension, the role of the Berry phase in resonance modes has been revealed both experimentally and theoretically, offering a guide for manipulating the ellipticities of circulating light waves and the resultant Berry phase in the range of π to 0.

The topological robustness of the Berry phase is a result of gauge invariance in the adiabatic evolution[34]. The Möbius waveguiding structures operate in the optical wavelength range and are of micrometre size, much smaller than those investigated in previous reports using helical waveguides and other open-light-path systems[15,16,35]. Such a miniaturized optical component is suitable for a new generation of on-chip integrable systems with excellent topological robustness for both fundamental physics and practical applications. The programming of optical 'Möbiosity' as a new route to light-topology shaping has the potential to serve as a versatile knob for all-optical manipulation of both classical bits and qubits, and implies promising functionalities such as supporting optical framed knots as information carriers[36], and quantum logic gates[37,38] in quantum computation and simulation.

Online content

Any methods, additional references, Nature Research reporting summaries, source data, extended data, supplementary information, acknowledgements, peer review information; details of author contributions and competing interests; and statements of data and code availability are available at https://doi.org/10.1038/s41566-022-01107-7.

References

1. Cohen, E. et al. Geometric phase from Aharonov–Bohm to Pancharatnam–Berry and beyond. *Nat. Rev. Phys.* **1**, 437–449 (2019).
2. Wang, J. & Zhang, S.-C. Topological states of condensed matter. *Nat. Mater.* **16**, 1062–1067 (2017).
3. Zhang, Y., Tan, Y.-W., Stormer, H. L. & Kim, P. Experimental observation of the quantum Hall effect and Berry's phase in graphene. *Nature* **438**, 201–204 (2005).
4. Xiao, M. et al. Geometric phase and band inversion in periodic acoustic systems. *Nat. Phys.* **11**, 240–244 (2015).
5. Sonoda, H. Berry's phase in chiral gauge theories. *Nucl. Phys. B* **266**, 410–422 (1986).
6. Datta, D. P. Geometric phase in vacuum instability: applications in quantum cosmology. *Phys. Rev. D* **48**, 5746–5750 (1993).
7. Yale, C. G. et al. Optical manipulation of the Berry phase in a solid-state spin qubit. *Nat. Photon.* **10**, 184–189 (2016).
8. Slussarenko, S. et al. Guiding light via geometric phases. *Nat. Photon.* **10**, 571–575 (2016).
9. Bliokh, K. Y., Rodríguez-Fortuño, F. J., Nori, F. & Zayats, A. V. Spin–orbit interactions of light. *Nat. Photon.* **9**, 796–808 (2015).
10. Pancharatnam, S. Generalized theory of interference, and its applications. *Proc. Indian Acad. Sci.* **44**, 247–262 (1956).
11. Berry, M. V. Quantal phase factors accompanying adiabatic changes. *Proc. R. Soc. London A* **392**, 45–57 (1984).
12. Berry, M. V. Interpreting the anholonomy of coiled light. *Nature* **326**, 277–278 (1987).
13. Berry, M. V. The adiabatic phase and Pancharatnam's phase for polarized light. *J. Mod. Opt.* **34**, 1401–1407 (1987).
14. Chiao, R. Y. & Wu, Y.-S. Manifestations of Berry's topological phase for the photon. *Phys. Rev. Lett.* **57**, 933–936 (1986).
15. Tomita, A. & Chiao, R. Y. Observation of Berry's topological phase by use of an optical fiber. *Phys. Rev. Lett.* **57**, 937–940 (1986).
16. Bliokh, K. Y., Niv, A., Kleiner, V. & Hasman, E. Geometrodynamics of spinning light. *Nat. Photon.* **2**, 748–753 (2008).
17. Liu, Y. et al. Circular-polarization-selective transmission induced by spin-orbit coupling in a helical tape waveguide. *Phys. Rev. Appl* **9**, 054033 (2018).
18. Patton, R. J. & Reano, R. M. Rotating polarization using Berry's phase in asymmetric silicon strip waveguides. *Opt. Lett.* **44**, 1166–1169 (2019).
19. Ma, L. B. et al. Spin–orbit coupling of light in asymmetric microcavities. *Nat. Commun.* **7**, 10983 (2016).
20. Xu, Q. et al. Electrically tunable optical polarization rotation on a silicon chip using Berry's phase. *Nat. Commun.* **5**, 5337 (2014).
21. Shao, Z. et al. Spin–orbit interaction of light induced by transverse spin angular momentum engineering. *Nat. Commun.* **9**, 926 (2018).
22. Tanda, S. et al. Crystal topology: a Möbius strip of single crystals. *Nature* **417**, 397–398 (2002).
23. Manoharan, H. C. Topological insulators: a romance with many dimensions. *Nat. Nanotechnol.* **5**, 477–479 (2010).
24. Demokritov, S. et al. Experimental observation of symmetry-breaking nonlinear modes in an active ring. *Nature* **426**, 159–162 (2003).
25. Rzepa, H. S. Möbius aromaticity and delocalization. *Chem. Rev.* **105**, 3697–3715 (2005).
26. Fomin, V. M., Kiravittaya, S. & Schmidt, O. G. Electron localization in inhomogeneous Möbius rings. *Phys. Rev. B* **86**, 195421 (2012).
27. Yin, Y. et al. Topology induced anomalous plasmon modes in metallic Möbius nanorings. *Laser Photon. Rev.* **11**, 1600219 (2017).
28. Bauer, T. et al. Observation of optical polarization Möbius strips. *Science* **347**, 964–966 (2015).
29. Song, Y. et al. Möbius strip microlasers: a testbed for non-Euclidean photonics. *Phys. Rev. Lett.* **127**, 203901 (2021).
30. Kreismann, J. & Hentschel, M. The optical Möbius strip cavity: tailoring geometric phases and far fields. *Europhys. Lett.* **121**, 24001 (2018).
31. Li, S. L. et al. Non-integer optical modes in a Möbius-ring resonator. Preprint at https://arxiv.org/abs/1311.7158 (2013).
32. Padgett, M. & Allen, L. Light with a twist in its tail. *Contemp. Phys.* **41**, 275–285 (2000).
33. Lei, F., Tkachenko, G., Ward, J. M. & Chormaic, S. N. Complete polarization control for a nanofiber waveguide using directional coupling. *Phys. Rev. Appl.* **11**, 064041 (2019).
34. Aharonov, Y. & Anandan, J. Phase change during a cyclic quantum evolution. *Phys. Rev. Lett.* **58**, 1593–1596 (1987).
35. Chiao, R. Y. et al. Observation of a topological phase by means of a nonplanar Mach-Zehnder interferometer. *Phys. Rev. Lett.* **60**, 1214–1217 (1988).
36. Larocque, H. et al. Optical framed knots as information carriers. *Nat. Commun.* **11**, 5119 (2020).
37. Jones, J. A., Vedral, V., Ekert, A. & Castagnoli, G. Geometric quantum computation using nuclear magnetic resonance. *Nature* **403**, 869–871 (2000).
38. Song, Y., Lim, J. & Ahn, J. Berry-phase gates for fast and robust control of atomic clock states. *Phys. Rev. Res.* **2**, 023045 (2020).

Methods

Numerical simulation

The 3D numerical simulations (COMSOL Multiphysics Wave Optics module) were carried out for both Möbius and curved strips. The key parameters were designed to meet the requirements for practical fabrication procedures and operation at telecommunication wavelengths (radius R = 10 µm, width of 0.9–4 µm and thickness of 0.6–1.5 µm). Models were generated using MATLAB with the equations provided in Supplementary Note 1. Optical-mode fields were simulated in the wavelength range 1,500–1,560 nm. IP and OP excitations were provided by a local line current source at the waveguide core oscillating along the corresponding directions. The local polarization state was extracted by analysing the electric-field distributions at the field maxima point of the waveguide's cross-section spanning from one mode antinode to node, and is presented using a projected polar plot.

Device fabrication

Pure quartz glass substrates were cleaned by immersion in acetone and isopropyl alcohol, ultrasonicated (Elmasonic S, Elma Schmidbauer), and dried with N_2 gas. The microcavities were fabricated using 3D direct laser writing (Photonic Professional GT, Nanoscribe) on cleaned quartz substrates. The laser lithography photoresist was dropcast onto the substrates. The principle of the direct laser writing system is based on multi-photon lithography and 3D scanning with a focused laser beam within the sample volume. A high-resolution galvanometer mirror system was used for laser-beam scanning in the x–y plane, which allowed each volumetric pixel to be positioned with an accuracy of 10 nm. The scanning was controlled by DeScribe software in Nanoscribe, which was also used to design the structures. During the fabrication process, the negative photoresist (IP-Dip, Nanoscribe) was polymerized by two-photon absorption (at 780 nm). After exposure, the structures were developed in mr-Developer (mr-Dev 600, Micro Resist Technology) followed by rinsing in isopropanol, which resulted in fabricated structures bonded onto the substrate. The structures were then dried using a critical point drier (Autosamdri-931, Tousimis Research Corporation) to remove the solvent. Each fabricated Möbius- and curved-strip microstructure was supported by two ~20-µm-high pylons to avoid optical leakage to the substrate.

Device characterization

For SEM imaging, the samples were sputter-coated with a thin (~8 nm) Cr layer to avoid charging and to improve contrast. The SEM images were acquired using an NVision40 system (Carl Zeiss) using a primary-beam energy of 5 keV. Optical transmission measurements were conducted using an evanescently coupled tapered fibre. The optical set-up and details of preparing the tapered fibre are provided in Supplementary Note 2. A wavelength-tunable infrared laser (Tunics 100S-HP, Yenista) was used as the light source, with a scanning range covering 1,500–1,600 nm. The transmission signal was measured using an InGaAs switchable-gain photodetector (PDA20CS-EC, Thorlabs). Resonances with a maximized extinction ratio of >10 dB were obtained by finely adjusting the coupling gap spacing. The polarization state of the incident laser light was controlled by a fibre-based three-paddle polarization controller. Launching of linearly polarized light with a tilted orientation was carefully examined by connecting a fibre-coupled polarimeter (PAX1000IR2, Thorlabs) at the output. Polarization mapping was carried out by adjusting the polarization angle of the input laser light in steps of 10°. The Berry phase was estimated by deriving the compensated phase value (that is, the resonant wavelength offset) for spectral matching of the resonance modes in Möbius- and curved-strip cavities with identical structural parameters.

Data availability

The main data supporting the findings of this study are available within the Supplementary Information. Additional data are available from the corresponding authors upon reasonable request.

Acknowledgements

We thank H. Xu and R. Engelhard for technical support and S. Kiravittaya for helpful discussions. L.M. acknowledges financial support from the Würzburg-Dresden Cluster of Excellence on Complexity and Topology in Quantum Matter–ct.qmat (EXC 2147, project-ID 390858490) and the German Research Foundation (MA 7968/2-1). O.G.S. acknowledges financial support from the Leibniz Program of the German Research Foundation (SCHM 1298/26-1). J.W. acknowledges support from the National Natural Science Foundation of China (grant no. 62105080). V.M.F. acknowledges financial support from the German Research Foundation (project no. FO 956/6-1).

Author contributions

L.M., O.G.S. and J.W. conceived the study, inspired by an initial investigation with S.L. and V.M.F. J.W., S.L., C.H.L., R.T. and V.M.F. performed the theoretical calculations and analysis. S.V., L.S. and M.M.-S. fabricated the samples. S.V. and J.W. conducted the optical experiments. S.B. conducted SEM characterizations. J.W., L.M., Y.Y. and S.L. analysed the data. J.W. and L.M. wrote the manuscript. All authors discussed the results and contributed to the manuscript.

Funding

Open access funding provided by Leibniz-Institut für Festkörper- und Werkstoffforschung Dresden (IFW).

Competing interests

The authors declare no competing interests.

Additional information

Supplementary information The online version contains supplementary material available at https://doi.org/10.1038/s41566-022-01107-7.

Correspondence and requests for materials should be addressed to Shilong Li or Libo Ma.

Peer review information *Nature Photonics* thanks Bruno Piccirillo and the other, anonymous, reviewer(s) for their contribution to the peer review of this work.